OVERVIEW

This paper presents a study of 16 models commonly used for the prediction of cooling-tower plume rise from natural-draft cooling towers by comparison with all available field data as of about 1980. This study forms the basis for the SACTI multiple tower model by establishing the most successful set of modeling approaches.

It was published in *Atmospheric Environment*, **Vol. 16**, No. 1, pp. 67-83, 1982.

Atmospheric Environment Vol. 16, No. 1, pp. 67–83, 1982
Printed in Great Britain.

0004-6981/82/010067-17 $03.00/0
Pergamon Press Ltd

EVALUATION OF MATHEMATICAL MODELS FOR NATURAL-DRAFT COOLING-TOWER PLUME DISPERSION

R. A. CARHART
Department of Physics, University of Illinois at Chicago Circle, Chicago, Illinois, U.S.A.

and

A. J. POLICASTRO and S. ZIEMER
Division of Environmental Impact Studies, Argonne National Laboratory, Argonne, U.S.A.

(*First received* 11 *December* 1979 *and in final form* 23 *October* 1980)

Abstract—This paper provides an evaluation of the theory and performance of 16 models commonly used for the prediction of cooling-tower plume rise from natural-draft cooling towers. The performance of the models is determined through model/data comparisons with: (a) field data encompassing visible plume outlines obtained through plume photographs and (b) single-phase laboratory data on plume trajectories and dilutions. The field data used included 39 data sets from single towers (Chalk Point, Lünen, Paradise) and 26 from multiple-towers (Neurath and Amos).

From the model/data comparisons carried out, six single-tower NDCT models and two multiple-tower NDCT models provided notably superior predictions than the remaining models. These models represent the current state of the art. For field-data applications, they can predict within a factor of two for visible plume rise and a factor of $2\frac{1}{2}$ for visible plume length, but only for 50% of the cases tested.

Our review of model assumptions, which included several sensitivity studies, revealed several problem areas which remain unresolved. First, no model is able to achieve correct simultaneous predictions of plume trajectory and dilution. Second, the common treatment of plume thermodynamics affects plume dynamics too strongly when ambient profiles favor plume conditional and/or ambient latent instability. Third, no model correctly represents the rapid bending and additional dilution exhibited by the data under high wind conditions. Fourth, the plume merging logic is oversimplified and does not account for the effects of wind direction on plume dispersion. Fifth, the treatment of the diffusion phase is not developed from data taken at the large heights these plumes attain.

The field and laboratory data base are sufficiently strong to support improvement in model theory and performance.

1. INTRODUCTION AND METHODOLOGY

The emphasis on closed-cycle cooling in the U.S. has increased the number of power plants being designed with natural-draft cooling towers (NDCTs). The prediction of the environmental impact of such towers has become an important part of the power-plant licensing process. Accurate modeling of the NDCT plumes is necessary to predict such impacts as drift deposition, plume shadowing, cloud generation and the aesthetic impacts of the visible plume. A rapid increase in the quality and quantity of experimental data on NDCT plumes in recent years has made it possible for us to carry out an extensive validation study of the numerous mathematical models that have been developed to predict the dispersion of NDCT plumes. Further details are presented in Policastro *et al.* (1980) and Carhart *et al.* (1978).

Most models currently in use for predicting cooling-tower plumes have been developed and calibrated using stack-plume data and/or laboratory water-plume data taken in a neutrally stratified crossflow. Despite the often-stated similarity between water plumes, stack plumes and NDCT plumes, the ranges of relevant dimensionless parameters differ significantly between categories. The fundamental nondimensional parameters that govern the dispersion of NDCT plumes are

$$F_0 = \frac{W_0}{\sqrt{g\frac{\rho_0 - \rho_a}{\rho_a}D}} \quad \text{(initial densimetric Froude number)} \tag{1}$$

$$k = \frac{U_0}{W_0} \quad \text{(velocity ratio)} \tag{2}$$

$$S = \left(\frac{D}{4U_0}\right)^2 \frac{g}{T_a}\frac{d\theta_a}{dz} \quad \text{(local ambient stability)}, \tag{3}$$

and

$$V^* = q_0 - q_a \text{ (ambient moisture deficit).} \tag{4}$$

Here W_0 is the tower exit velocity; U_0 is the wind speed at the tower top; D is the tower exit diameter; θ_a is the ambient potential temperature and ρ_0 and ρ_a are, respectively, the tower exit density and ambient density at the tower top, including moisture effects. The quantities q_0 and q_a are the exit plume and ambient specific humidities, respectively. Exit Reynolds numbers are sufficiently high to indicate fully developed turbulent flow and independence of exact value.

For NDCT plumes, F_0 generally varies between 0.4 and 0.9, making such plumes considerably more buoyant than stack plumes, mechanical-draft cooling-tower (MDCT) plumes, or thermal plumes in water. Also, the k values for NDCT plumes range from 0 to 5, with $k > 1.0$ most of the time. Few stack or water plumes have k values above 1.0. Even without mentioning differences in the S and V^* parameters, NDCT plumes represent a unique range of F_0 and k values, representing a class of plumes with high buoyancy and generally strong crossflow. Due to the unique range in F_0 and k for NDCT plumes, it is important to test the validity of the commonly made assumptions in existing NDCT models through model/data comparisons complemented with critical theoretical evaluations. Further, the comparative study of a large number of existing models with experimental data has the additional benefit of identifying those models that can best be used to predict NDCT plumes in environmental-impact assessments.

A search of the literature yielded the following data as most suitable for model evaluation:

(a) Field data at five sites covering visible plume outlines from photographs, detailed ambient profiles, and tower exit conditions (39 data sets for single NDCT plumes and 26 data sets for multiple NDCT plumes). See Bremer *et al.* (1973), Slawson and Coleman (1978), Meyer (1975), Meyer and Jenkins (1977), Baer *et al.* (1974) and Kramer *et al.* (1975, 1976).

(b) Single-phase laboratory data taken at Electricité de France (EDF) by Viollet (1977) covering a range of F_0 and k values appropriate to NDCT plumes. The data were acquired in a water plume under isothermal ambient conditions (corresponding to neutral stratification in air) with a scale-model tower structure present in the flow to simulate tower downwash conditions that occur in the field.

All models evaluated in this paper were compared with the field data; only the better-performing models were compared with the laboratory data to test the validity of the physical assumptions employed in those models.

The laboratory data employed in model testing were acquired from parametric studies in which a range in k values is employed for each F_0. These single-phase data can accurately represent the near-field processes of entrainment and momentum transfer and possibly tower downwash effects under carefully controlled conditions. The field data, however, include the physical effects operational in the near and far fields. Among the effects occurring in the field which are not represented by the lab data include:

(1) ambient turbulence (unmeasured magnitude) of importance in the far field,

(2) ambient profile variability with time and horizonal position and

(3) thermodynamics processes of condensation and evaporation.

We can see then that the laboratory and field data provide complementary information.

Ideal field-data for model validation purposes consists of time-averaged visible plume outlines, time-averaged tower exit conditions, and single or time-averaged on-site ambient profiles of temperature, humidity, wind speed and wind direction. Figure 1 summarizes the sites and the corresponding tower characteristics where field data are available. The data cover a range of installations from small heat and moisture output (Lünen) to large heat and moisture output (Amos). The visible-plume outlines give direct information on the *trajectory* of the plume as well as indirect information on *dilution* (from the final plume length and rise). Most field-data cases at these sites were not complete. Profiles were sometimes taken off-site, and some cases contained only one profile, which prevented time-averaging. Tower outlet conditions had to be inferred for some cases. In other cases, the time correlation between various parts of the data was not close. A more complete review of the data for each site and their uncertainties can be found in Policastro *et al.* (1980). However, for the present study the quality of these data sets was sufficient for model testing purposes. Our use of visible-plume data revealed important systematic behaviors in the predictions of most models which we were able to trace to model assumptions.

Plant name and/or location	No. of towers	Generator maximum power and tower geometry
Lünen, West Germany	1	335 MWe; H = 109.3 m; R_0 = 25.7 m
Chalk Point, Maryland	1	600 MWe; H = 124.1 m; R_0 = 27.4 m
Paradise, Kentucky	1*	1100 MWe; H = 132.8 m; R_0 = 30.9 m
Neurath, West Germany	3	H = 100 m; R_0 = 22.3 m; 300 MWe; 60°; 114 m; 60° 60°; 300 MWe; 300 MWe
John E. Amos, West Virginia	3†	H = 132 m, 150 m; R_0 = 29.0 m, 39.5 m; 1300 MWe; 187 m; 800 MWe; 166°; 188 m; 800 MWe

Fig. 1. Source geometry and maximum generator load cooled by towers at the three single-tower sites and the two multiple-tower sites where field data were acquired.

All models tested in this paper are of the one-dimensional integral or semiempirical type, commonly used in environmental-impact evaluation (see Fig. 2). The models studied are described by Batty (1976); Calabrese *et al.* (1974); Frick (1975); Hanna (1975); LaVerne (1976); Lee (1977); Orville *et al.* (1975); Moore (1977); Saame (1971); Slawson and Coleman (1977); Stephen and Moroz (1972); Tsai and Huang (1972); Weil (1974); Slawson and Wigley (1975) and Winiarski and Frick (1976, 1978). A summary of the assumptions included in each model is given in Table 1.

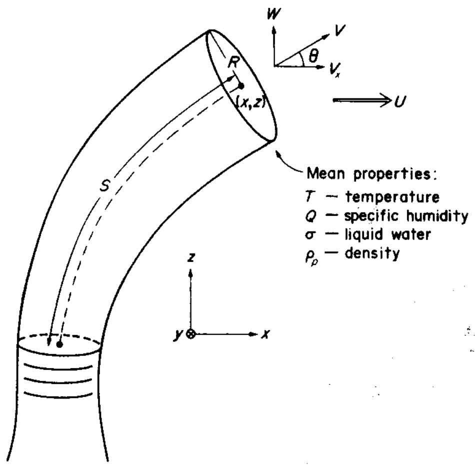

Fig. 2. Definition of symbols used to describe plume shape and velocity.

Finite-difference models were not considered because they are not presently used for impact studies.

2. BASIC PROCESSES IN COOLING-TOWER PLUME DISPERSION

The dispersion of a cooling-tower plume will first be discussed qualitatively to emphasize the unique aspects of its behavior. At the tower mouth a highly buoyant turbulent jet enters the ambient crossflow. For a short distance beyond the exit plane the plume has a uniform flow "potential core", which decreases in lateral extent as the turbulent mixing region moves closer to the centerline. At the end of this zone of flow establishment (ZFE), the potential core disappears and the centerline values of plume properties begin to decrease. Thereafter the profiles have a "horseshoe" shape due to the pair of counterrotating vortices that develop, as observed by Fan (1967) and Viollet (1977).

The enhanced buoyancy in an NDCT plume causes increased turbulent mixing and strengthens the vortex pair and its associated mixing, as compared to a pure jet ($F_0 = \infty$). Despite the actual complexity of the flow, most modelers assume azimuthally symmetric

Table 1. Summary of major assumptions made in each of the 16 single-NDCT and the seven multiple-NDCT plume models included in the study

Model	Closed-form or integral? (C, I)	Boussinesq approximation? (Y, N)	Gaussian or top-hat profiles? (G, T)	Circular or elliptical section? (C, E)	All profiles same width? (Y, N)	Bentover plume assumpt., $V_x = u$? (Y, N)	Drag force? (Y, N)	Thermodynamics or simple mixing? (T, M)	Modified buoyancy term? (Y, N)	Separate atmospheric diff. logic? (Y, N)	Explicit downwash effects? (Y, N)	Handles multiple towers? (Y, N)
Calabrese–Halitsky–Woodard	C		G	E	Y					Y	N	Y
Frick	I	Y	T	E	Y	N	N	T	N	Y	N	N
Hanna	I	Y	T	C	N	Y	N	T	Y	N	N	Y
KUMULUS	I	N	G	E	Y	Y	N	T	N	Y	Y	Y
Lee (NUS)	I	N	G	C	Y	N	Y	T	N	N	N	Y
Lee–Batty	I	N	T	C	Y	Y	N	T	N	Y	N	N
ORFAD	C		G	E	Y					Y	N	Y
Orville	I	Y	T	C	Y	Y	N	T	N	Y	N	Y
Saame	C		G	E	Y					Y	N	N
Slawson (closed form)	C	Y	T	C	Y	Y	N	S	N	Y	Y	N
Slawson–Wigley	I	N	T	C	Y	Y	N	S	N	Y	N	Y
Stephen–Moroz	I	N	T	C	Y	Y	N	T	N	N	N	N
Tsai–Huang (S and W)	I	Y	G	C	Y	N	Y	S	N	N	N	N
Weil	I	N	T	C	Y	N	N	T	N	N	N	N
Winiarski–Frick	I	N	TG	C	Y	N	N	T	N	N	N	N
Winiarski–Frick (1977)	I	N	T	C	Y	N	Y	T	Y	N	N	N

Gaussian or tophat profiles, and attempt to represent vortex-pair mixing by a suitably chosen entrainment function.

In a pure jet, the vertical velocity decreases monotonically as the mass flux increases. However, because buoyancy acts to increase the vertical velocity, an NDCT plume actually accelerates in the vertical direction initially. Later, as dilution reduces the buoyancy, the plume's vertical velocity also decreases. Thus, velocity shear persists longer, the entrainment rate is increased, and the plume trajectory bends over more slowly compared to a nonbuoyant jet with the same exit velocity and diameter.

Many investigators consider there to be a significant pressure drag force on both jets and plumes in a crosswind due to the pressure difference between the windward and the leeward sides of the jet or plume. In this view, the plume behaves somewhat like an obstacle inclined to the crossflow. The assumed force acts to decrease the plume's vertical velocity and increase its horizontal velocity. Because a buoyant plume bends over more slowly than a pure jet, the effect of such a force on a buoyant plume would be enhanced, compared to its strength for a jet with the same k value.

Thermodynamic processes that occur because of the presence of recondensate droplets and water vapor in an NDCT plume, help to identify the plume trajectory and an outline of the plume. These processes are, of course, absent from single-phase buoyant or nonbuoyant flows. If a moist plume is subsaturated, its adiabatic lapse rate is nearly dry adiabatic; and its behavior approximates that of a single-phase buoyant plume. However, as a saturated parcel rises and cools, water vapor must condense and release latent heat, because the saturation mixing ratio decreases with temperature. If the parcel stays just *at* saturation, the released heat reduces the rate of cooling with rise to the saturated adiabatic lapse rate, ($0.65\,\mathrm{K}\,(100\,\mathrm{m})^{-1}$ at 0°C, but only $0.35\,\mathrm{K}\,(100\,\mathrm{m})^{-1}$ at 30°C).

The relationship between the adiabatic lapse rates of the plume and the ambient determines whether the plume rise is stable (buoyancy reduced by rise) or unstable (buoyancy increased by rise). For saturated plumes the dividing line can be as low as $0.35\,\mathrm{K}\,(100\,\mathrm{m})^{-1}$ and depends strongly on temperature. The ambient can thus be stable for the rise of a dry plume and unstable for the rise of a saturated plume, a behavior called *conditional instability*. When present under humid conditions, conditional instability can lead to very long and high visible plumes.

An additional atmospheric condition, well known to meteorologists in studies of cloud formation is *ambient latent instability*. This type of instability sometimes enhances the effects of plume conditional instability. If one lifts a parcel of ambient air without mixing, at some height the parcel will have both condensed moisture and positive buoyancy (level of free convection (LFC)). Above the LFC, the parcel will rise unstably. Since it takes energy to raise the parcel to this height, the parcel at ground level is said to possess *latent instability;* the less energy required, the greater the parcel's latent instability. A rising cooling-tower plume can provide this energy by entraining ambient air and carrying it upward.

Although the identity of the "parcel" disappears when it is mixed with plume air, the tendency of entrained air to contribute strongly to large visible plumes increases with its degree of latent instability. Since ambient conditions with high latent instability often favor plume conditional instability as well, the effects usually reinforce one another. These thermodynâmic effects on the rise of the plume can be dramatic under conditions of low wind, near neutral stability and small saturation deficits.

Late in plume dispersion the plume's velocity vector has become nearly that of the ambient. Turbulence due to velocity shear and vortex circulation no longer dilute the plume substantially. Mixing during this phase of plume development, the atmospheric phase, is dominated by diffusion due to the background ambient turbulence, due to the fact that excess plume properties (values above ambient) in this regime are close to their corresponding ambient values. Experimentally, little is known about the nature of atmospheric turbulence at heights of 200–1000 m above the ground.

3. UNRESOLVED ISSUES IN THE MODELING OF NDCT PLUMES

In this section we discuss five areas in which there remains controversy on the physically correct assumptions. Our purpose is to identify problem areas and to indicate how the models giving the best predictions handle each problem. These five areas are: (a) the balance between momentum transfer and dilution mechanisms; (b) the nature of correct moisture thermodynamics; (c) the effects of the tower wake on trajectory and dilution; (d) the formulation of the atmospheric diffusion phase and (e) the representation of the plume merging process.

(a) *The balance between momentum transfer and dilution mechanisms*

The most important factor in predicting plume evolution accurately is the mass entrainment rate, which governs the rate of dilution of plume properties. All models assume that entrained ambient air adds to the plume all of its horizontal momentum. The models also assume an Archimedes-type buoyancy force acting on the plume, even though the plume is certainly not static. Thus, without any other forces that transfer momentum to the plume but do not directly alter plume dilution, the relationship between the dilution rate of the plume and its rate of bendover is determined.

Any model that only included buoyancy and entrainment as momentum-transfer mechanisms was unable to predict both plume length and plume trajectory. More momentum transfer (bending) is needed for a given dilution (length). Even those models assuming a drag force revealed this difficulty.

Unless one uses simultaneous dilution and trajectory data to test existing models, the full seriousness of this trade-off may not be evident. Special mechanisms were present in the better-performing models to help alleviate this problem, three of which are the following:

(1) *The bent-over-plume assumption.* In this assumption the plume horizontal velocity equals the ambient velocity at all heights, including at the tower exit. Thus, an immediate increase in plume horizontal momentum occurs without any accompanying dilution. This assumption, then, provides more bendover for the same dilution, which helps to restore the needed balance. Even if valid, the physical basis for this assumption has not been clarified. However, if one includes the bent-over-plume assumption, the usual buoyant force acting vertically, and properly adjusted entrainment coefficients so that plume dilutions are correct, then plume trajectories are still not sufficiently bent over with the wind. Such behavior emphasizes the difficulty of resolving the dilution/momentum-transfer conflict in a physically believable manner.

(2) *Different spreading rates for momentum and temperature.* The Hanna model assumes that the rate of spread of momentum is larger than the rate of spread of temperature, based on considerations by Briggs (1975). The smaller spread of temperature than momentum implies that a smaller buoyancy force (determined from the temperature plume) will operate on a larger mass (determined from the momentum plume). This effectively reduces the buoyancy acting on the jet, leading to more rapid plume bendover. The Hanna model shows good trajectories and reasonable dilutions for $k < 1.5$ in predicting the single-phase EDF cases.

(3) *Lengthening of visible portion of plume by means of nontophat distributions.* The Winiarski–Frick model assumes no drag force and does not make the bent-over-plume assumption. As expected, their tophat-equivalent model for plume variables defined as cross-sectional averages predicts a rapidly overdiluted plume with early evaporation of liquid water. The tendency is then reversed by appealing to the assumed cosine distributions, which lead to a saturated core, even when the average water vapor is subsaturated at the average temperature at a particular plume cross section. That this view of the plume is not entirely successful is shown by this model's persistent, if mild, tendency to underpredict plume length.

To verify our evaluation of the mechanisms behind the predictive trends for visible plume data, we tested predicted trajectories and dilutions of three of the better performing models with laboratory data. Chosen were the Hanna and Winiarski–Frick models (two of the most accurate models for single NDCT visible plume length) and the Slawson–Wigley model (widely known). The laboratory data were taken by EDF in a neutrally stratified water flume. The Froude number, F_0, was varied between 0.4 and 50; and k ranged from 0.5 to 5.0. A scale model of the hyperbolic tower structure provided simulation of wake effects. A fluorescein dye tracer was used for dilution measurements.

The performance of each model in predicting trajectory and dilution was consistent with the model's behavior for those same quantities in our visible plume data. For example, Fig. 3 shows a typical case with $F_0 = 0.8$ and $k = 1.0$. The Hanna and Winiarski–Frick model trajectories agree well with the observed trajectory. However, the Winiarski–Frick model predicts too great a dilution, consistent with its mild tendency to underpredict visible plume length. The Hanna model predicts too little dilution, consistent with its moderate tendency to overpredict visible plume length. The Slawson–Wigley model assumes no drag forces and is apparently not calibrated optimally. The predicted plume trajectory lies above the observed one, and the plume dilutes too slowly. Increasing the model's entrainment coefficient would improve both predictions.

In summary, then, one must regard this first modeling issue as still unresolved. The correct balance between momentum transfer by drag forces, entrainment, and the action of buoyancy still needs to be specified to give both correct trajectories and correct dilutions as the plume develops. Supplementary in-plume velocity data for dispersing cooling-tower plumes would aid in resolving this question.

(b) *Moisture thermodynamics*

Except for models that did not account for liquid water separately (Slawson–Wigley, Saame), all models make the equilibrium assumption that as entrained ambient air mixes with plume air and supersaturates or subsaturates the plume, an immediate condensation or evaporation occurs to maintain the plume at saturation. If Q_p represents the average specific humidity of the plume, Q_S the saturation specific humidity, T the average plume temperature and p the pressure at a given height, then this assumption can be written

$$Q_p = Q_s(T, p). \tag{5}$$

The average amount of liquid water in the plume has an initial value at the tower exit. It is an additional dependent variable, which changes in accord with conservation of enthalpy, conservation of total water, and Equation 5.

The main physical effect of these thermodynamic assumptions in a model is that, instead of cooling with adiabatic rise at a rate close to the dry adiabatic lapse rate, the plume cools at the slower saturated adiabatic lapse rate, γ_s. This lapse rate is a strong function of temperature, ranging for most locations from 0.3 to 0.7 $K\ (100\,m)^{-1}$.

Under most atmospheric conditions the inclusion or omission of thermodynamics has little effect on the plume predictions of a model. However, in the 10–20% of field cases where thermodynamics is important,

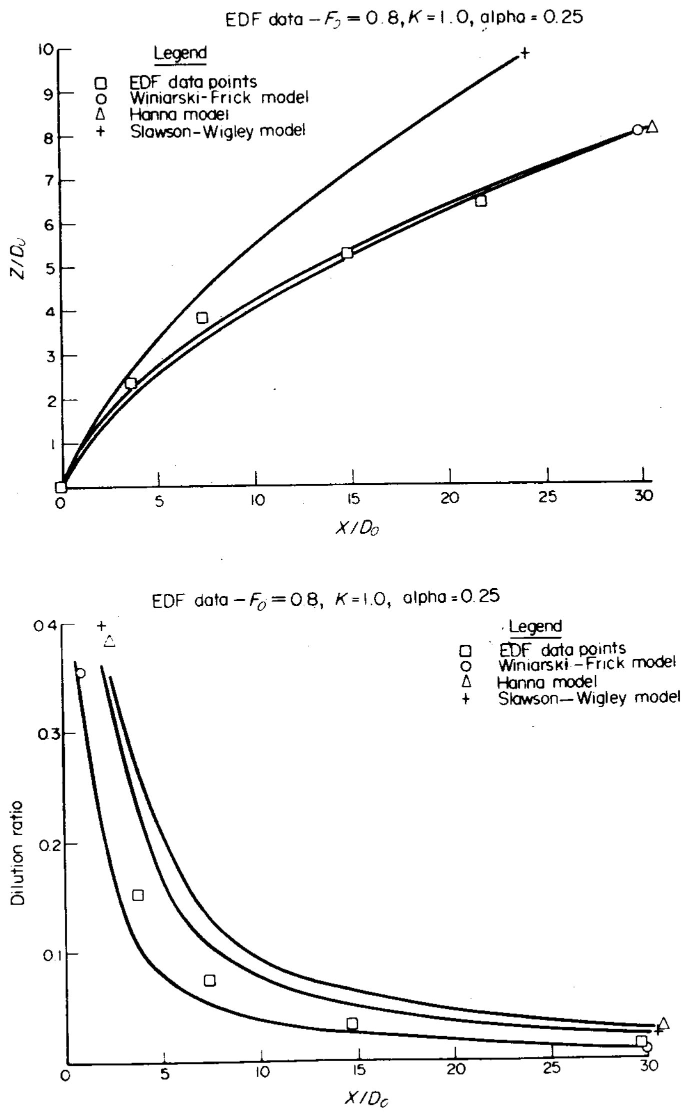

Fig. 3. Comparison of model predictions of the Winiarski–Frick, Hanna, and Slawson–Wigley models to Electricite de France (EDF) laboratory data on: (a) trajectory and (b) dilution; data for a moderate cross-flow-to-exit-velocity ratio. The alpha value refers to the exponent in the power-law velocity profile with respect to height above the "ground," x is the downwind distance, and z is the distance above the tower.

both plume trajectory and plume length predictions are very sensitive to thermodynamic assumptions. We found that models which use the equilibrium assumption and allow liquid–water and thermodynamic effects to occur across the entire temperature plume will overestimate these effects substantially. On the other hand, models that treat the sum of liquid and vapor water as a passive tracer with no thermodynamics cannot predict some of the very large plumes that result when thermodynamic effects are important.

As discussed earlier, thermodynamics has important effects when ambient profiles indicate that plume conditional instability or ambient latent instability, or both can occur. Strong plume conditional instability occurs under low winds, high relative humidities and ambient temperature stratifications from mildly stable ($\approx 0.5\,K\,(100\,m)^{-1}$) to unstable. Large ambient latent instability results whenever the ambient has high relative humidity and near-neutral temperature stratification. When either or both of these instabilities were favored by ambient conditions and a model adopting the equilibrium theory across the entire temperature plume was used, the predicted plumes tended to be long and high. Also, the data generally show extensive plumes under these ambient conditions. However, models that ignore moisture thermodynamics, assuming total water is a passive tracer, often failed to predict large observed plumes.

Figure 4 illustrates a field case at Paradise in which the observed plume shows the effects of these instabilities. Here ambient stratification is unstable up to 100 m above the tower, with isothermal conditions above that height. Due to the low ambient temperatures, the moderate ambient relative humidities correspond to saturation deficits that are small (less than 1 g kg^{-1}). The resulting large plume is a clear example of the ability of moisture-related instabilities to produce a large visible plume volume. The relative stability of the ambient suggests that plume conditional instability is the primary effect.

The model predictions shown in Fig. 4 also deserve comment. The Weil-model prediction is short and low with a reasonable predicted trajectory. The model uses full equilibrium thermodynamics. In this case, however, the excessive dilution chosen for the model prevents any realization of moisture-related instabilities. The Frick model's short, low prediction arises partly from overdilution. But both the Winiarski–Frick and Frick models tend not to exhibit effects of moisture-related instabilities for another reason, as well. Although they intend to use full equilibrium thermodynamics, the actual algorithm chosen for the computer code leads to a significant loss of liquid water. This loss helps prevent the prediction of a large plume in this case and generally shortens other plume predictions.

A more dramatic effect of the use of full equilibrium thermodynamics can be seen in Fig. 5 for the Weil model (cf. with Fig. 4.). The entrainment rate used in the Weil model is so large that the model's predictions are normally very short. However, in this case, which exhibits both instabilities, the model *overpredicts* plume length. Even gross overdilution is insufficient to eliminate the effects of the instabilities. It appears, then, that the modeling of moisture thermodynamics across the entire plume cross section produces effects that are too extreme. Other graphical comparisons of the Weil model show the same, very instructive, behavior (Policastro *et al.*, 1980).

One might conclude then that a neglect of thermodynamics altogether would be a better assumption. In fact, models that did this still predicted extensive visible plumes in cases where ambient latent instability is high. But they failed to predict extensive plumes when only plume conditional instability was present. For example, Fig. 6 shows the Slawson–Wigley model prediction for the same case as Fig. 4, a case in which ambient latent instability is important. This model includes no thermodynamics. However, in a similar case when plume conditional instability is the dominant mechanism, shown in Fig. 7, the Slawson–Wigley model gives a very short visible plume prediction. The complete absence of moisture thermodynamics in the governing equations is thus also seen to be too extreme for NDCT plume prediction.

As with the first unresolved issue, the most successful models each incorporated mechanisms to avoid either of these extremes. Two of the mechanisms were:

(1) *Use of different spreading rates for moisture and temperature.* The Hanna model followed the spirit of equilibrium thermodynamics, but assumed that thermodynamic effects occurred over only about half of the temperature-elevated portion of the plume cross section. The cross-sectional area of the moisture plume is reduced by this technique, but the total fluxes of liquid water and water vapor are unaffected. As a result, the moisture perturbations are larger by a factor of R^2 (temperature plume)/R^2 (moisture plume). That

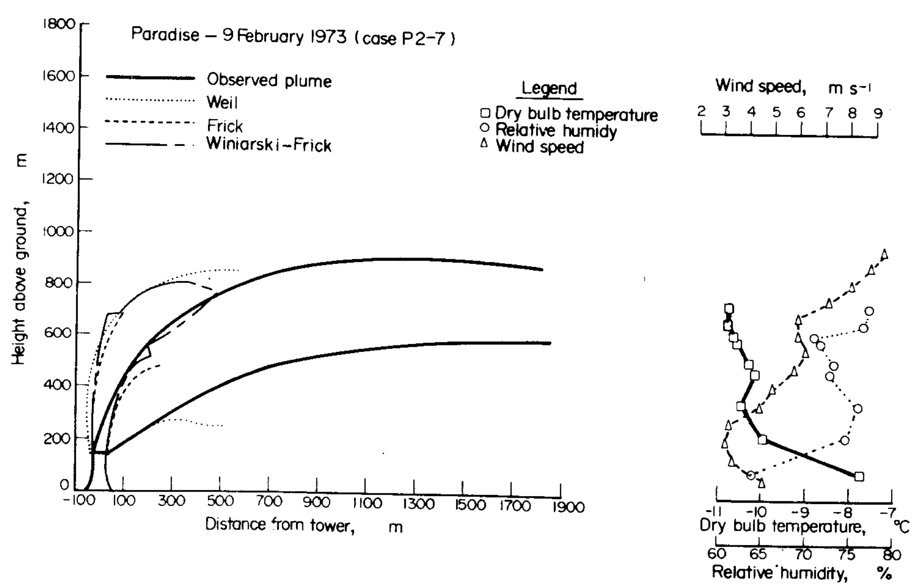

Fig. 4. Single-NDCT plume predictions of the Weil, Frick and Winiarski–Frick models for a field data case with weakly stable, low saturation-deficit ambient conditions and moderate winds. This data case exhibits primarily plume conditional instability in the observed plume.

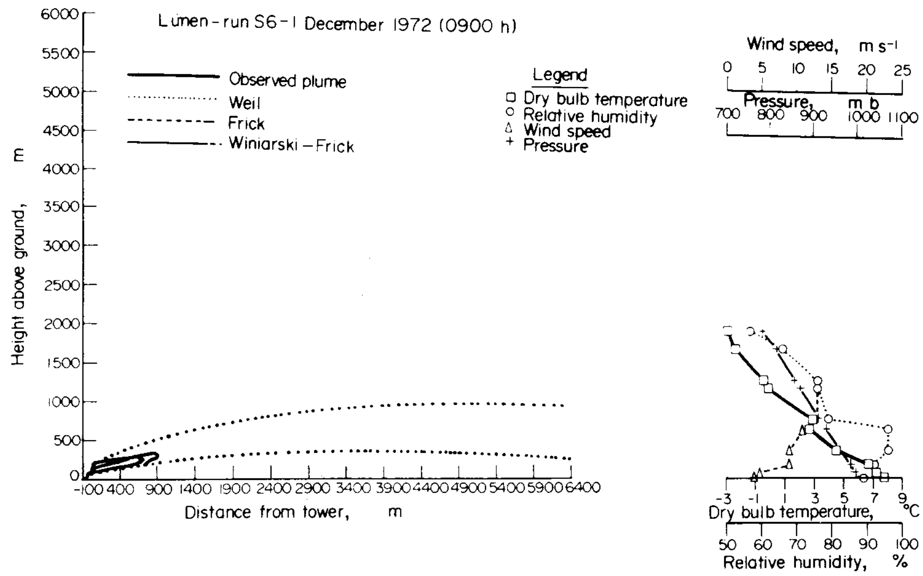

Fig. 5. Single-NDCT plume prediction of the Weil model for near-neutral, low-saturation-deficit ambient conditions showing excessive effects of both moisture-related instabilities in the prediction.

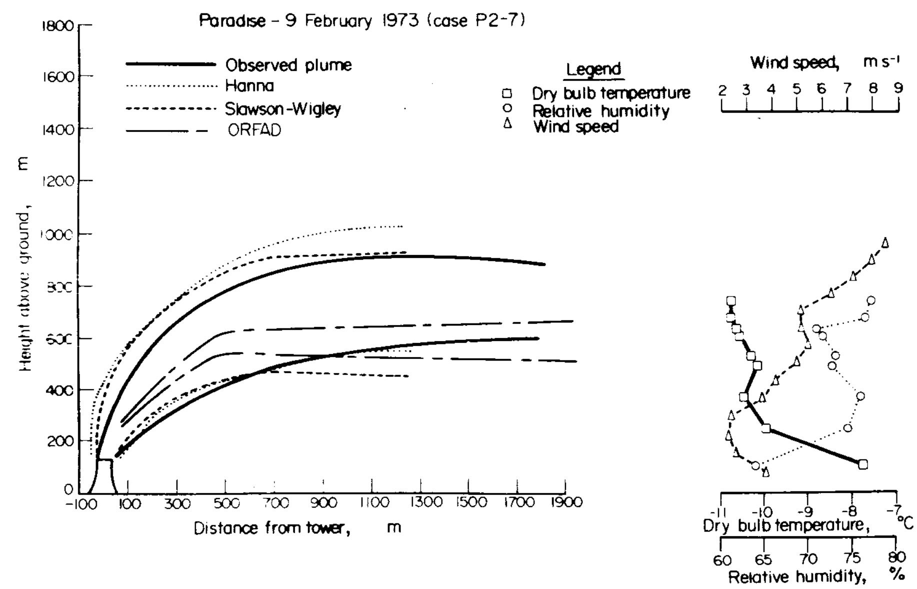

Fig. 6. Single-NDCT plume prediction of the Slawson–Wigley model for a case with near-neutral, low saturation-deficit ambient conditions and low winds, showing the model's ability to represent effects of ambient latent instability.

assumption clearly reduces the degree of thermodynamic effects. It leads to less plume conditional instability because the plume lapse rate lies between the dry adiabatic and saturated adiabatic lapse rates. The physical basis offered for this assumption is that the moisture occurs in pockets inhomogeneously across the temperature plume. But detailed experimental evidence will be needed to verify this picture, especially with the use of a moisture-plume area that is exactly half the temperature-plume area in all cases.

(2) *Use of nontophat distributions.* In the Winiarski–Frick model, a large entrainment rate is assumed, which leads to overdilution of average plume properties and early disappearance of liquid water as discussed above. Beyond this point the average plume mixing ratio drops below saturation at average plume

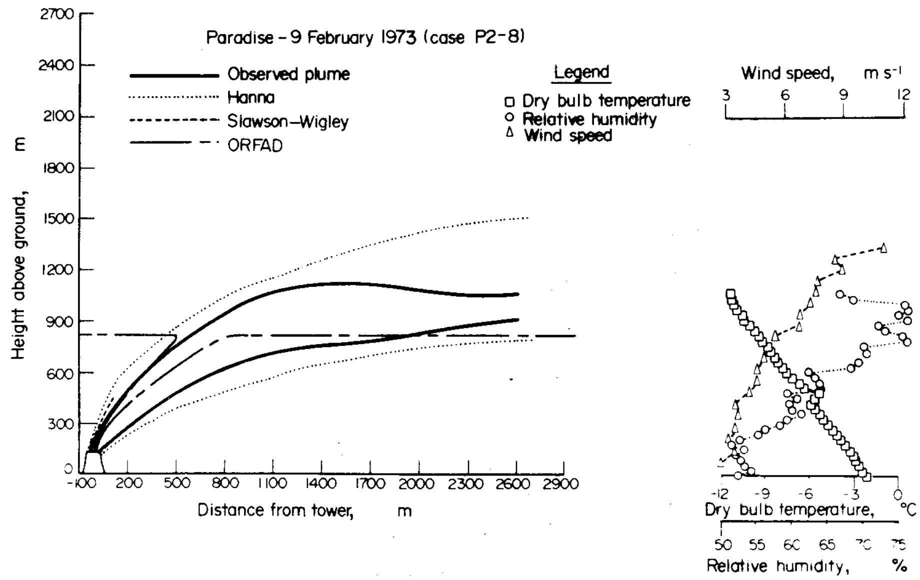

Fig. 7. Single-NDCT plume prediction of the Slawson–Wigley model for a case with near-neutral ambient temperature stratification, low winds, and moderate saturation deficits above 700 m, exhibiting the model's inability to represent effects of plume conditional instability.

temperature. However, the assumed cosine profiles of temperature and mixing ratio in the plume cross-section will peak at the plume centerline so as to yield a supersaturated central "core", resulting from the non-linearity of the saturation curve.

Considerable additional mixing (a 3.37-fold increase in mass flux) is necessary with the assumed distributions of temperature and water vapor to subsaturate the plume at its centerline. No thermodynamics are included after the average properties become subsaturated. The Winiarski–Frick procedure markedly extends the visible portion of the plume, but also effectively eliminates the occurrence of plume conditional instability in the predictions. The model's predictions are usually quite short for long plumes. Thus, this method for reducing thermodynamic effects in plume predictions in order to agree with observations is only partially successful.

We conclude, therefore, that the nature and degree of thermodynamic effects on a dispersing NDCT plume is still unsettled. The validity of the two methods of avoiding large thermodynamic effects is not clear. In-plume moisture and temperature measurements would help to resolve these issues.

(c) *Effect of the tower wake on trajectory and dilution*

As the ambient crossflow encounters the tower structure, it produces a wake downwind of that obstacle. The wake exhibits decreased pressure, but increased turbulence intensity. A plume emitted from the tower is generally affected in two ways by the tower wake. First, the increased pressure differential between the upwind and lee sides of the tower exerts a force on the plume which tends to bend it over more rapidly, and may even bend it below the tower mouth. Second, the increased turbulence intensity in the wake causes greater-than-normal entrainment and more rapid dilution when the plume trajectory is low enough for a plume/wake interaction to occur strongly. (We refer to these effects generically as downwash effects.)

Tower-wake effects for large winds are important as a result of an analysis of our field and laboratory data. Of the time-averaged visible plume outlines for the 39 single-tower NDCT data sets, the 10 cases where $k > 1.5$ have plume outlines and/or centerlines that drop below the tower exit plane near the tower. Further, the EDF laboratory data show that, for $F_0 = 0.8$ and $k > 1.5$, the tower wake causes increased dilution and lower trajectories as compared to expected dilutions and trajectories extrapolated from low-to-moderate wind values. Thirteen of the 15 models studied ignore tower-wake effects altogether. In reality, downwash due to the tower structure is not a physical phenomenon that can be treated consistently within the integral approach, since integral methods implicitly assume no boundary interference. However, empirical formulations can be added to simulate the effect of the wake and will hopefully prove adequate.

The two models that attempt an empirical treatment of downwash are the KUMULUS and Slawson (Closed Form) models. The KUMULUS model includes an additional downward force acting on the plume and assumes additional entrainment. However, in the Slawson model, only the trajectory is modified by means of an empirically fitted downwash constant in the trajectory equation. That constant was obtained through calibration of model predictions to the 13 Paradise cases used in this study. The trajectory constant also modifies the effective entrainment rate, because, as used, it affects radial growth. Unfortunately, Slawson's treatment of downwash seems to reduce radial growth and dilution rather than enhance it; however, trajectories are definitely lowered.

Figure 8 shows a dramatic effect of the omission of wake effects in most models. The data are replotted from the EDF laboratory tests with $F_0 = 0.8$ and k varying from 0.5 to 3.0, where the presence of a scale model of the tower produces a realistic wake.

In Fig. 8 the downwind distance at which a factor-of-10 dilution occurs is plotted against k with all other parameters fixed. Note that, as k begins to increase, the factor-of-10 dilution occurs farther downwind until about $k \simeq 1.7$, beyond which it occurs increasingly closer to the tower. This latter decrease happens because the lower plume trajectory allows the plume to experience increased turbulent mixing in the tower wake. None of the three models shown exhibit this trend, as one would expect given the absence of a tower-wake formulation in the models. The Slawson (Closed Form) model is not presented here because its downwash effects are turned off in neutral stratifications, having been calibrated only for cases from very stable to near neutral. The effect of tower downwash on plume trajectory is shown in Fig. 9. When this figure is compared with Fig. 3, one can see that models whose trajectory predictions were good for $k = 1$ generally predict trajectories that bend over too slowly at high k; and all models shown underdilute. Thus, downwash effects are the third important area of NDCT plume modeling needing better development.

(d) *Atmospheric diffusion formulations*

Atmospheric turbulent diffusion emerges as the main mechanism for further mixing and dilution of the

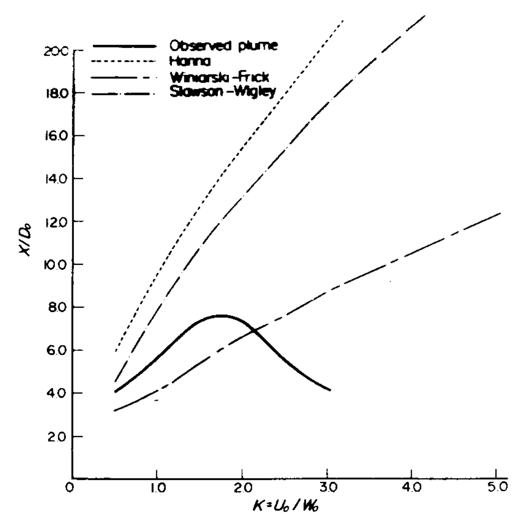

Fig. 8. Comparison of downwind distance in tower diameters at which 10:1 dilution of tower effluent occurs as a function of k. Results of EDF laboratory data are compared with predictions of the Hanna, Winiarski–Frick and Slawson–Wigley models.

plume as its buoyancy and velocity relative to the wind approach zero. Then the plume properties become nearly passive tracers for further turbulent diffusion. Differences between the formulations chosen for different models were of several types.

(1) Some models assumed turbulent diffusion throughout plume rise; others included this type of mixing only after some criterion was met, related to the plume's becoming passive in the ambient environment.

(2) Different criteria were chosen to initiate the atmospheric diffusion phase, such as the updraft velocity vanishing, or the plume slope falling below a standard small value.

(3) Modelers selected different cross-sectional shapes for the diffusion phase, different spreading rates, and different dependences of both on ambient stability.

Ten of the 39 single-NDCT plumes and most of the multiple-NDCT cases at Amos show visible plumes beyond the point where the trajectory has leveled off. Omission of a treatment of atmospheric diffusion seriously affects a model's ability to treat this type of plume. For this reason, the models by Hanna and by Stephen and Moroz could not provide definite plume-length predictions for many of the cases.

Seven of the 15 models, however, did include a separate means for calculating atmospheric diffusion of the plume. Except for the Lee–Batty model, all incorporated the work of Pasquill (1962) in some form, using Gaussian distributions of plume variables. The Gaussian widths are a function of downwind distance and atmospheric stability class.

We cannot establish the validity of this type of method simply from the model/data comparisons for the relevant cases, because other sources of model variability caused widely differing diffusion-phase results with the same type of method. For instance, the use of different criteria for entering the diffusion phase led to different initial conditions for atmospheric diffusion for the same case. Also, there were inherent differences between model predictions for the rising phase of plume dispersion, giving differing initial conditions for the diffusion phase.

Pasquill's methods may not be applicable above about 200 m and particularly within elevated inversions. However, their use in the final stage of plume dispersion or the identification of superior alternatives clearly merits further testing and study. Atmospheric diffusion data at heights above 200 m are needed as a basis for more reliable formulations.

(e) *Methods for plume merging*

Plants with more than one NDCT require the modeling of the merging of plumes from separate towers into a combined plume. When plumes merge, their circumference-to-area ratio decreases, and their total entrainment rate decreased below the cumulative entrainment rate of the previously unmerged plumes. Thus, relative to the unmerged plumes, the effects of buoyancy are increased and dilution is reduced, delay-

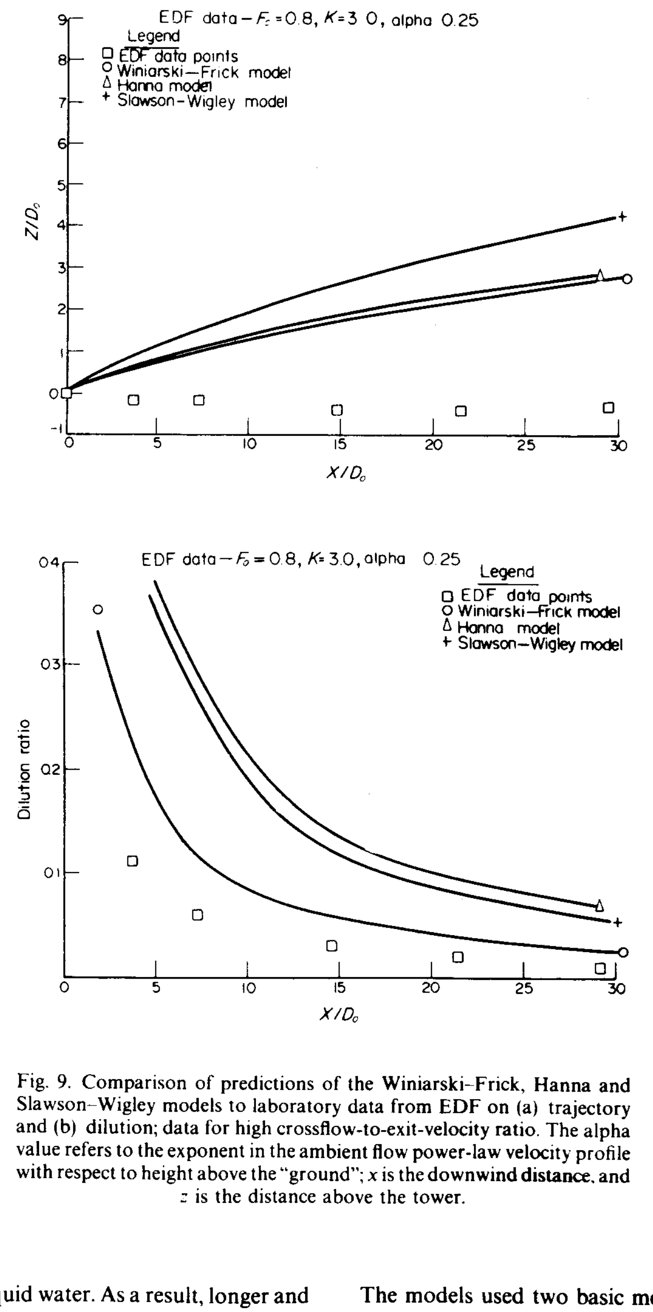

Fig. 9. Comparison of predictions of the Winiarski-Frick, Hanna and Slawson-Wigley models to laboratory data from EDF on (a) trajectory and (b) dilution; data for high crossflow-to-exit-velocity ratio. The alpha value refers to the exponent in the ambient flow power-law velocity profile with respect to height above the "ground"; x is the downwind distance, and z is the distance above the tower.

ing evaporation of liquid water. As a result, longer and higher-rising plumes can be expected when plumes merge.

Only six of the 15 models studied were formulated to handle multiple-source configurations. The methods used, while not fully satisfying from a physical point of view, did partially represent the enhanced buoyancy and slowed dilution expected for merged plumes. But none included the effects of wind direction relative to the configuration of sources, which can be important. We selected 26 multiple-NDCT cases from Neurath and Amos to test the predictions of these six models. Typical predictions of each model are shown in Figs 10 and 11.

The models used two basic merging methods:

(1) The Orville and Calabrese-Halitsky-Woodard models specify an effective source, as though the plumes were merged into a singular circular cross-section plume in the exit plane. The fluxes of the merged plume are matched to the summed fluxes of the individual sources.

(2) The Lee, Hanna and Slawson-Wigley models adopt the most realistic method used. The primary (largest) plume is followed according to the single NDCT submodel until its radius grows to half the separation distance to the nearest tower. Then the plumes are all merged suddenly into a single round plume, which has the same total fluxes of mass,

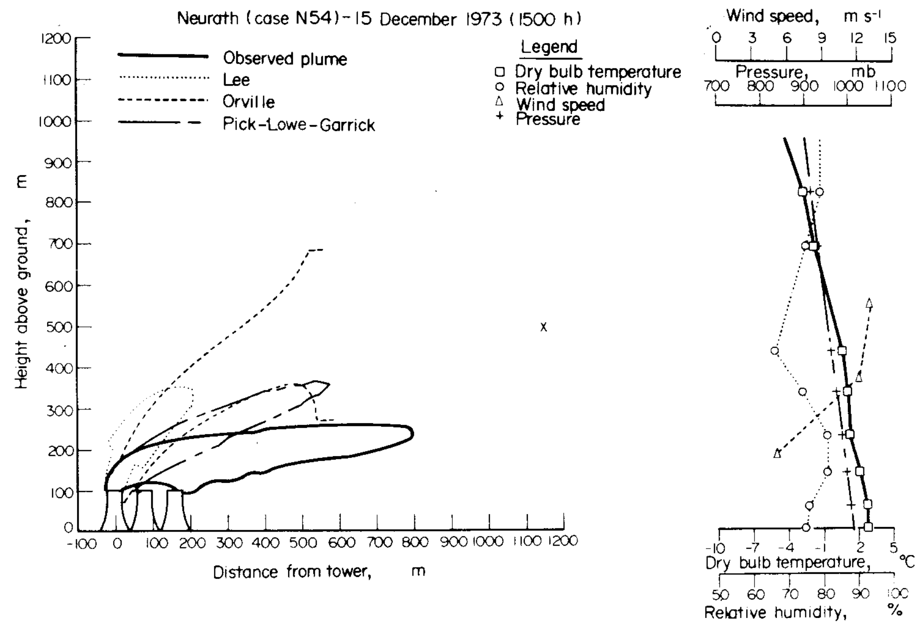

Fig. 10. Typical multiple-NDCT plume predictions of the Lee, Orville and Calabrese–Halitsky–Woodard (Pickard–Lowe–Garrick) models.

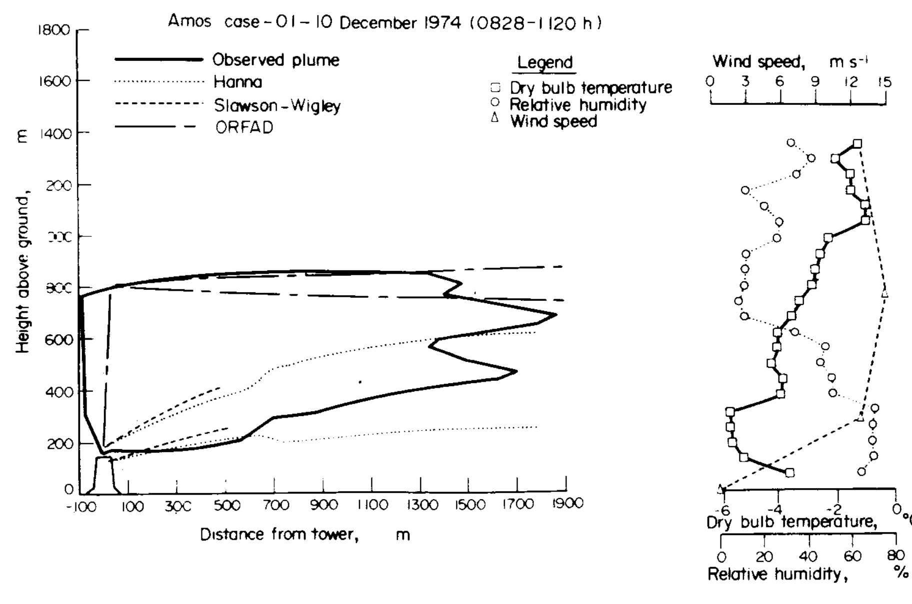

Fig. 11. Typical multiple-NDCT plume predictions of the Hanna, Slawson–Wigley and ORFAD models.

momentum, enthalpy and water. Since the larger cumulative entrainment and dilution typical of the separate sources is allowed to persist longer than with method (1), the procedure gives plumes that dilute and bend over faster.

Because of the differences between the formulations of the six models, the relative merits of these two approaches cannot be evaluated from the model/data comparisons alone, since the variations in predictive performance between the models due to differing assumptions mask the more subtle differences caused by choice of merging logic. If our data base included source geometries where the tower centers were spaced more widely than 2 or 3 diameters, the difference between the last two methods would probably be more pronounced in the model/data comparisons.

Model performance statistics for all six models were worse for the 26 multiple-NDCT cases than for the 39 single-NDCT cases. Perhaps none of the three approaches is an adequate approximate representation of the actual merging process. It may be that neglect of wind-direction effects, failure to use a three-dimensional picture to determine "nearness" of the unmerged plumes, and failure to represent sequential merging of individual plumes in appropriate geometries (rather than simultaneous merging of all individual plumes in one cross section) are the inadequacies leading to the predictive degradation noted. We believe the effects of wind direction on the merging of plumes are significant and should be included in multiple-tower models. However, the Amos subset (75%) of multiple-tower data cases has the greatest uncertainties associated with it; and also for these cases the atmospheric diffusion phase formulation plays a proportionately larger role than it does for single-tower cases. Thus, some caution must be shown in trying to attribute the performance degradation of models noted above to the treatment of merging of plumes.

4. DISCUSSION OF MODEL PERFORMANCE

Another prime goal of this study is to specify the degree of accuracy achieved in these currently available models for predicting the extent of visible plumes from NDCT installations. Quantitative characterizations of model performance were obtained by computation of selected model-performance statistics. In the following, ρ represents the ratio of predicted plume length (or rise) to observed plume length (or rise). Table 3 shows the set of model performance statistical measures we selected for single-NDCT cases and Table 4 shows the same measures for multiple-NDCT cases. The rationale for use of each specific measure will be discussed first, and then categories of predictive accuracy will be presented in terms of these statistics.

The *range* of ρ_i illustrates the predictive extremes to which the model was subject. The integer N_F records the number of cases for which the model could not be used because conditions for its application were not met. For example, the Hanna, Stephen–Moroz and Lee models failed to give a definite length prediction in any case in which the plume was still visible when the updraft velocity first vanished. However, these models gave definite rise predictions in such a case. Thus, N_F for plume length was incremented by one, but N_F for plume rise was not.

Given the uncertainties of the data and the results of sensitivity studies we carried out, a prediction within a factor of two should be considered a "good" prediction. The integer N_2 measures the number of predictions whose ρ value lies between 0.5 and 2.0. In interpreting this statistic, one must remember that a prediction can qualify within a factor of two on length and not on rise or vice-versa. For length only, $N_{2.5}$ is also tabulated, because model length predictions were generally somewhat less accurate than rise predictions.

The final integer measure, N_5, is somewhat arbitrary. Predictions outside a factor of 5 were considered "misses"; but if a definite prediction resulted, it was not considered a case where the model is inapplicable, and was not included in N_F. Values of ρ outside a factor of 5 were omitted in the calculation of

Table 2. Characterization of the predictive trends noted from model/data comparisons for each of the 16 models included in the study

Model	Predictive trend
* Calabrese–Halitsky–Woodard (PLG)	Balanced, but tends to overpredict length and rise for moderate-length plumes
Frick	Extreme length underprediction, substantial rise underprediction.
* Hanna	Balanced rise predictions; tends to overpredict length in low winds, high humidities
* KUMULUS (Motor Columbus)	Balanced, but slightly underpredicts rise for long multiple-tower plumes
* Lee (NUS)	Balanced for plume rise; very short for plume length
Lee–Batty	Extreme length underprediction, substantial rise underprediction
* ORFAD	Very long and high, if a prediction is made at all
* Orville	Overpredicts length and rise for single towers, more balanced for multiple towers
Saame	Substantial length and rise underprediction
Slawson (Closed Form)	Balanced length and rise predictions
* Slawson–Wigley	Underpredicts plume length and rise
Stephen–Moroz	Moderate overprediction for rise; tends to underpredict long plumes
Tsai–Huang (S and W)	Tends to underpredict rise when observed rises far; severely overpredicts length of long plumes
Weil	Usually strongly underpredicts length and rise; but overpredicts both in near-neutral, humid conditions
Winiarski–Frick	Substantial length underprediction for long plumes; slight rise underprediction
Winiarski–Frick 77	Substantial length underprediction; moderate rise underprediction

* Indicates the model handles multiple towers also.

Table 3. Performance statistics for 16 single-tower models based on visible plume rise and visible plume length in 39 field data cases

Model	Range of ρ_i	N_2	N_5	N_F	$\bar{\rho}_1 = \frac{1}{n}\sum\rho_i$	σ_1	$\bar{\rho}_2 = 10^{1/n\sum\|\log\rho_i\|}$	σ_2
Visible Plume Rise								
Slawson–Wigley	0.01–6.78	17	30	0	0.83	0.68	1.89	0.20
Slawson (closed form)	0.01–7.38	20	32	0	0.96	0.71	1.77	0.18
Weil	0.09–6.07	16	32	0	0.74	0.64	2.05	0.19
Frick	0.07–3.83	16	37	0	0.61	0.59	2.19	0.20
Winiarski–Frick	0.13–6.50	31	37	0	0.83	0.36	1.49	0.13
Winiarski–Frick (1977)	0.10–4.79	24	37	0	0.70	0.71	1.86	0.15
ORFAD	0.56–7.93	5	11	27	2.34	1.29	2.27	0.19
Hanna	0.23–11.00	30	38	0	1.27	0.82	1.60	0.16
Tsai–Huang (Stone and Webster Engr. Corp.)	0.01–10.57	24	32	0	0.92	0.49	1.52	0.14
Lee–Batty	0.11–9.96	19	32	1	0.92	0.75	1.88	0.23
Lee (NUS)	0.21–12.97	29	38	0	1.09	0.67	1.64	0.17
Calabrese–Halitsky–Woodard (Pickard–Lowe–Garrick Inc.)	0.10–10.61	18	29	8	1.52	1.01	1.86	0.18
Stephen–Moroz	0.23–20.52	24	35	0	1.44	0.97	1.68	0.19
Saame	0.47–9.70	17	36	2	2.08	0.94	2.01	0.17
Orville	0.44–34.87	23	35	0	1.74	1.20	1.78	0.20
KUMULUS	0.03–2.60	27	35	1	0.95	0.49	1.50	0.14

Model	Range of ρ_i	N_2	$N_{2.5}$	N_5	N_F	$\bar{\rho}_1 = \frac{1}{n}\sum\rho_i$	σ_1	$\bar{\rho}_2 = 10^{1/n\sum\|\log\rho_i\|}$	σ_2
Visible plume Length									
Slawson–Wigley	0.00–6.50	7	11	24	0	0.72	0.77	2.33	0.19
Slawson (closed form)	0.00–22.87	13	19	27	0	1.15	1.09	2.12	0.17
Weil	0.01–24.27	5	7	19	0	0.52	0.54	2.85	0.19
Frick	0.03–0.61	3	4	15	0	0.36	0.13	2.99	0.15
Winiarski–Frick	0.08–2.39	23	27	33	0	0.79	0.49	1.77	0.15
Winiarski–Frick (1977)	0.06–1.79	14	20	30	0	0.66	0.45	2.11	0.20
ORFAD	0.32–16.18	0	0	2	17	2.49	2.17	3.79	0.09
Hanna	0.19–2.90	21	23	27	11	1.21	0.71	1.57	0.15
Tsai–Huang (Stone and Webster Engr. Corp.)	0.01–4.90	19	21	28	6	1.68	1.08	1.81	0.19
Lee–Batty	0.00–3.93	8	14	24	2	0.85	0.90	2.27	0.15
Lee (NUS)	0.00–0.94	5	7	21	2	0.41	0.22	2.76	0.20
Calabrese–Halitsky–Woodard (Pickard–Lowe–Garrick Inc.)	0.04–541	13	19	27	8	1.27	0.95	1.90	0.17
Stephen–Moroz	0.10–383	16	18	23	13	1.41	0.98	1.60	0.19
Saame	0.09–24.35	11	19	28	2	0.75	0.81	2.21	0.15
Orville	0.27–17.04	20	23	32	0	1.72	1.22	1.72	0.22
KUMULUS	0.01–75.38	27	30	33	1	1.11	0.80	1.59	0.16

Notes:
ρ_i is defined as the ratio of predicted to observed (either length or height as indicated).
N_2 is the number of times the prediction is within a factor of 2, i.e., $0.5 < \rho_i < 2.0$.
$N_{2.5}$ is the number of times the prediction is within a factor of 2.5, i.e., $0.4 < \rho_i < 2.5$.
N_5 is the number of times the prediction is within a factor of 5, i.e., $0.2 < \rho_i < 5.0$.
N_F is the number of failures of the model in 39 data sets.
σ_1 is the standard deviation of the ρ_i distribution.
σ_2 is the standard deviation of the $|\log \rho_i|$ distribution.

mean ρ values, so as not to mask predictive trends by occasional serious mispredictions.

Finally, two different mean ρ values were computed for model length predictions and rise predictions separately. The usual arithmetic mean, $\bar{\rho}_1$, and its standard deviation, σ_1, gives evidence of systematic overprediction, underprediction or balanced under- and overprediction. The second mean, $\bar{\rho}_2$, is the log mean, which tends to deemphasize the substantial misses. In comparing the $\bar{\rho}$ values tabulated for the models, we must consider N_5 along with them, because a model with a large N_5 may be penalized for moderate mispredictions, while another model may have a small N_5 but good ρ values for that small subset of the data.

Because users of NDCT plume models have differing goals, it is not possible to single out one or several of these statistics, or to form a single combined measure of performance, in order to rank the models in a way suitable for all users. Much more can be learned from a careful comparative study of Tables 3 and 4 than can be learned from a simple ranking of models for predictive accuracy, or even a grouping of them. But to summarize the predictive ability of state-of-the-art models for single-NDCT visible plumes, we have

Table 4. Performance statistics for seven multiple-tower models based on visible plume rise and visible plume length in 26 field data cases

Model	Range of ρ_i	N_2	N_5	N_F	$\bar{\rho}_1$	σ_1	$\bar{\rho}_2$	σ_2
Visible Plume Rise								
Hanna	0.24–5.50	19	25	0	1.17	0.63	1.51	0.15
Slawson–Wigley	0.12–3.27	13	20	0	0.98	0.71	1.71	0.16
ORFAD	0.44–3.73	0	3	23	2.07	1.34	2.58	0.11
Lee (NUS)	0.19–7.25	19	24	0	1.10	0.50	1.56	0.14
Orville	0.38–66.25	18	25	0	1.59	1.06	1.72	0.18
Calabrese–Halitsky–Woodard (Pickard–Lowe–Garrick Inc.)	0.23–2.31	9	17	9	0.92	0.62	1.84	0.21
KUMULUS	0.21–1.81	19	25	1	0.83	0.42	1.64	0.21

Model	Range of ρ_i	N_2	$N_{2.5}$	N_5	N_F	$\bar{\rho}_1$	σ_1	$\bar{\rho}_2$	σ_2
Visible Plume Length									
Hanna	0.08–3.03	9	9	11	13	1.05	0.69	1.54	0.18
Slawson–Wigley	0.01–2.46	5	8	13	0	0.80	0.67	2.24	0.19
ORFAD	14.42–39.46	0	0	0	23	0.0	0.0	1.0	0.0
Lee (NUS)	0.0–1.20	2	2	7	6	0.48	0.39	2.89	0.27
Orville	0.02–21.83	11	14	18	1	0.93	0.67	1.84	0.19
Calabrese–Halitsky–Woodard (Pickard–Lower–Garrick Inc.)	0.03–1.06	7	7	10	9	0.69	0.29	1.67	0.23
KUMULUS	0.03–4.61	10	13	23	1	1.34	1.20	2.17	0.20

Notes:
ρ_i is defined as the ratio of predicted to observed (either length or height as indicated).
N_2 is the number of times the prediction is within a factor of 2, i.e., $0.5 < \rho_i < 2.0$.
$N_{2.5}$ is the number of times the prediction is within a factor of 2.5, i.e., $0.4 < \rho_i < 2.5$.
N_5 is the number of times the prediction is within a factor of 5, i.e., $0.2 < \rho_1 < 5.0$.
N_F is the number of failures of the model in 26 data sets.
σ_1 is the standard deviation of the ρ_i distribution.
σ_2 is the standard deviation of the $|\log \rho_i|$ distribution.

adopted the following criterion, which seems to emerge naturally from the predictive accuracy of the better-performing models: for half of the cases model predictions are within a factor of 2 for visible plume rise and a factor of $2\frac{1}{2}$ for visible plume length. The models of Hanna, Motor Columbus (KUMULUS), Orville, Slawson (Closed Form), Tsai and Huang (Stone and Webster), and Winiarski and Frick satisfy this criterion. Their performance for the prediction of visible plume outlines is also best upon examination of our complete set of graphs similar to those in Figs 4–7. The graphical comparisons and performance statistics of the Frick and ORFAD models show overall poor performance. All other models tested provide comparatively fair predictions.

For predicting multiple-NDCT visible plumes, we used the same criterion to express the state-of-the-art predictive capability of models for the Neurath and Amos cases. The models of Motor Columbus (KUMULUS) and Orville satisfy this criterion. The models of Hanna, Slawson and Wigley, and Lee can predict visible plume height within a factor of 2 at least 50% of the time, but they fail to predict visible plume length adequately, partly for reasons detailed above. The Calabrese–Halitsky–Woodard and ORFAD models showed overall statistically poor performance in predicting both visible plume length and rise for the multiple-NDCT cases.

In general, the models that performed best for single and multiple tower sites seem to be those that were calibrated to field data. The Hanna model was calibrated to data from the Amos site. KUMULUS was calibrated to our entire data base. Earlier runs we received from Motor Columbus based on prior calibration of KUMULUS showed a systematic overprediction of visible plume rise with our data. Slawson adjusted the coefficients in his model based on the 13 Paradise cases, which were his measurements. The Orville model was calibrated to mechanical-draft tower data from Benning Road, collected by Meyer *et al.* (1975). The most striking evidence on this point comes from the Winiarski–Frick model. The 1977 version of the model was calibrated to laboratory trajectory data and gave performance statistics as shown in Table 3. Currently, the model is reformulated and recalibrated on the basis of our single-NDCT data. The level of improvement in model performance achieved when a large field database was used is evident from the Table 3 values for the two Winiarski–Frick models.

5. SUMMARY AND CONCLUSIONS

Sixteen mathematical models for visible-plume prediction from natural-draft cooling towers are evaluated theoretically and tested with 39 sets of single-tower visible-plume field data from three sites

(Paradise, Kentucky; Chalk Point, Maryland and Lünen, West Germany). Seven of these models with the capability of treating plumes from multiple towers are further tested with 26 sets of multiple-tower data from two sites (Amos, West Virginia and Neurath, West Germany). The visible plume outlines provided by these data give information on the trajectory of the plume as well as dilution (from the final plume length and rise). Single-phase laboratory data on NDCT plumes were also used to supplement these data allowing us to test some aspects of model behavior under selected sets of ambient conditions. The model/data comparisons prepared for this study revealed systematic behaviors in the predictions of most models which we were able to trace to model assumptions.

A wide range of predictions occurred among the models. Six single-tower models [Hanna, KUMULUS, Orville, Slawson (Closed Form), Stone and Webster, and Winiarski and Frick] and two multiple-tower models (KUMULUS and Orville) performed best based on the criterion that visible-plume-length predictions be within a factor of 2.5 and visible-plume-height predictions be within a factor of 2 of the observed in at least 50% of all cases tested. No model has performed consistently well for all data sets. The better performance of the competitive models is partly due to the fact that most of them (except Stone and Webster) have been calibrated with field data.

Model/data discrepancies are partly due to model errors and partly to data-measurement errors. The level of accuracy of the data (ambient profiles, tower exit conditions, and visible plume outlines) makes it unlikely for a model to predict better than a factor of 1.5–2 in most data cases.

Our theoretical analysis of the model formulations revealed that models that correctly predict the plume trajectory due to the entrainment mechanism alone will overpredict dilution. The addition of a pressure drag force or use of the bent-over-plume assumption is helpful, but does not completely correct the problem of accurately providing both trajectory and dilution. The highly buoyant nature of NDCT plumes may not be modeled accurately in the theoretical formulations.

A second area of common difficulty lies in the treatment of plume thermodynamics. Numerical studies show that, in 10–20% of our field data cases, the feedback effects of thermodynamics on dynamics are important. In such cases, plume conditional and/or ambient latent instability is important. Unfortunately, when these effects prevail, their treatment by models yields too severe an impact due to thermodynamics (generally too large and voluminous plumes are predicted). In-plume data on liquid-water content and lateral extent would help greatly to clarify which assumptions are most correct. A recent study by Coulter (1979) of the relationship between the sizes of the temperature and moisture plumes is a step in this direction.

A third problem area relates to the effect of tower downwash. Laboratory and field data show that at moderate-to-high winds there is (a) an additional pressure force pulling the plume downward into the tower wake and (b) additional entrainment due to plume interaction with the turbulent tower wake. Only two of the 16 models evaluated attempt to account for these effects. In general, models predict a relatively small dilution (at fixed distances downwind) under high wind conditions, instead of the very large dilution that actually occurs. This erroneous behavior is systematic in all models we tested.

The fourth problem area relates to plume merging. Simplistic methods such as the "equivalent source" method ignore effects of wind direction on the rate of entrainment during plume merging. Finally, the treatment of the atmospheric diffusion place is generally empirical and lacks data on plume dispersion 200–1000 m high under differing ambient stabilities.

It is interesting that the more successful models employ mechanisms (correct or not) that attempt to respond to the first two problem issues. The more successful models employ an additional mechanism to provide additional bending without additional mixing. They also incorporate some mechanisms for reducing, but not eliminating, moisture thermodynamics. The correctness of *any of these* additional bending mechanisms remains to be determined.

Improved predictions for single- and multiple-tower NDCT plumes can be made by improving model assumptions by resolving the above issues. As a practical matter any of the models studied would perform better with our database if the model were calibrated on the basis of these data. An analysis of the lab and field data for systematic behaviors will help define trends to be predicted by the models. Once better model assumptions are defined, a calibration of the improved model to laboratory and field data can be accomplished. The data base encompassing lab and field data are sufficiently strong, consistent, and diversified to permit such improvement.

Acknowledgements—The authors wish to express their appreciation to the developers of the 16 models studied here. Each provided extensive cooperation by providing us with his computer codes and supporting documentation, and by resolving questions arising from the use of the models with our data base. We also appreciate the efforts of the developers of the proprietary Pickard–Lowe–Garrick and Motor Columbus (KUMULUS) models who prepared model predictions for us for our field data cases. The authors are grateful to Mr. Kent Haake for producing most of the graphical comparisons that provided the basis for this study.

The work here was supported by the U.S. Nuclear Regulatory Commission under Contract No. NRC-40-10-01-06-1 (Mr. Robert Abbey, Project Manager) and by the Electric Power Research Institute under Contract No. RP 906-1 (Dr. John Bartz, Project Manager) with Argonne National Laboratory. Finally, partial computer support was given by the University of Illinois at Chicago Circle Computer Center on their IBM/370–158 computer.

REFERENCES

Abraham G. (1971) The flow of round, buoyant jets issuing vertically into ambient fluid flowing in a horizontal direction. Delft Hydraulics Laboratory. Delft, The Netherlands, Publication No. 81.

Baer *et al.* (1974) Untersuchung an einem Naturzug-Nasskühlturm, Verein Deutscher Ingenieure, Fortschritts-Bericht der VDI Zeitschrift, Reihe 15, Nr. 5, Juli 1974.

Batty K. B. (1976) Sensitivity tests with a vapor plume model applied to cooling tower effluents. Master's Thesis, Dept. of Meteorology, Penn. State University.

Bremer *et al.* (1973) Bericht über die meteorologische Messerie am Standort Lünen vom 27. 11. 1972 Zur Teilüberprüfung und Verfeinerung des numerischen Modells SAUNA, Arbeitsgruppe uber die meteorologischen Auswirkunger der Kühltürme, Dienst für Luftreinhaltung der Schweizerischen Meteorologischen Zentralanstalt, Payerne.

Briggs G. A. (1975) Plume rise. In *Proceedings of the Workshop on Meteorological and Environmental Assessment*, American Meteorological Society, Boston, Mass. (See also *Plume Rise*, AEC Critical Review Series, USAEC Report TID-25075, Nov. 1969.)

Calabrese R. V., Halitsky J. and Woodard K. (1974) Prediction of temperature and moisture distributions in cooling tower plumes. In *Symposium on Atmospheric Diffusion and Air Pollution*, 9–13 *Sept.* 1974. American Meteorological Society, Boston, Mass.

Carhart R. A., Policastro A. J., Ziemer S. and Haake K. (1978) Critical review of thirteen models for plume dispersion from natural draft cooling towers. In *Proceedings of the Second Waste Heat Management and Utilization Conference, Miami Beach*, FL. Available from NTIS, PB80-112311 and PB80-112329.

Coulter R. L. (1979), Some turbulence and diffusion parameter estimates within cooling tower plumes derived from sodar data. *J. appl. Met.* in press.

Fan L. N. (1967) Turbulent buoyant jets into stratified or flowing ambient fluids. W. M. Keck Lab. of Hyd. and Water Res.. Report No. KH-R-18, California Institute of Technology, Pasadena, CA.

Frick W. E. (1975) The influence of stratification on plume structure. Master's thesis, Atmospheric Sciences Dept., Oregon State University.

Hanna S. R. (1975) Predicted and observed cooling tower plume rise and visible plume length at the John E. Amos power plant. *Atmospheric Environment* **10**, 1043–1052.

Kramer M. L. *et al.* (1975) John E. Amos cooling tower flight program data, Dec 1974–March 1975. American Electric Power Service Corp.

Kramer M. L. *et al.* (1976) John E. Amos cooling tower flight program data, Dec. 1975–March 1976, American Electric Power Service Corp.

LaVerne M. E. (1976) *Oak Ridge Fog and Drift Program (ORFAD) User's Manual*, ORNL/*TM*-5021, Oak Ridge National Laboratory, Oak Ridge, Tenn.

Lee J. L. (1977) Potential weather modification from cooling tower effluents at conceptual power parks. *Atmospheric Environment* **11**, 749–759.

List E. J. and Imberger J. (1973) Turbulent entrainment in buoyant jets and plumes, *J. Hydraulics Div. ASCE*, **99**, (HY9), 1461–1474.

Meyer J. H. *et al.*(1975) Mechanical-draft cooling tower visible plume behavior – measurements, models, predictions, cooling tower environment–1974. U.S. Energy Research and Development Administration, CONF-740302, 307–352.

Meyer J. H. (1975) Chalk point surface weather and ambient atmospheric profile data, first intensive test period, December 15–19, 1975 (revision). Applied Physics Lab., John Hopkins Univ., PPSP-CPCTP-4REV (and Environmental Systems Corps. document PPSP-CPCTP-8.)

Meyer J. H. and Jenkins W. R. (1977) Chalk point surface weather and ambient atmospheric profile data, second intensive test period, June 14–24, 1976. Applied Physics Lab., John Hopkins Univ., PPSP-CPCTP-11; (and Environmental Systems Corp. document PPSP-CPCTP-12).

Moore R. D. (1977) *The KUMULUS Model for Plume and Drift Deposition Calculations for Indian Point Unit No. 2*, Environmental Systems Corp., Knoxville.

Orville H. D., Hirsch J. H. and May L. E. (1975) Application of a cloud model to cooling tower plumes and clouds *J. appl. Met.* (in press).

Pasquill F. (1962) *Atmospheric Diffusion*, Van Nostrand Monographs, London.

Policastro A. J., Carhart R. A., Ziemer S. and Haake K. (1980) *Evaluation of Mechanical Models for Characterizing Plume Behavior from Cooling Towers. Vol.* 1. *Dispersion from Single and Multiple Source Natural Dfaft Cooling Towers.* U.S. Nuclear Regulatory Commission Report NUREG/CR-1581 (Vol. 1)

Policastro A. J., Carhart R. A., Ziemer S. E. and Haake K.. (1979) *Evaluation of Mathematical Models for Single and Multiple Source Natural-Draft Cooling Tower Plume Dispersion*, NUREG CR 1581, Vol. 1, U.S. Nuclear Regulatory Commission, 1–493.

Saame J. (1971) An analytical investigation of the formation and dispersion of fog plumes from a natural draft water cooling tower for various meteorological conditions. Master's thesis, Dept. of Mechanical Engineering, University of Pittsburgh.

Slawson P. R. and Coleman J. H. (1978) Natural-draft cooling-tower plume behavior at Paradise steam plant. Part II. Tennessee Valley Authority. Division of Environmental Planning, TVA/EP-78-01. February 1978.

Slawson P. R. and Coleman J. H. (1977) *Natural-Draft Cooling-Tower Plume Behavior at Paradise Steam Plant, Waste Heat Management and Utilization*, Vol. III. Hemisphere Publishing Corp., Washington, DC.

Slawson P. R. and Wigley P. M. (1975) The effects of atmospheric conditions on the length of visible cooling tower plumes. *Atmospheric Environment* **9**, 437–445.

Stephen D. W. and Moroz W. J. (1972) Plume rise from wet cooling towers in strong winds. Engineering Research Bulletin B-107, Center for Air Environment Studies, Penn. State University.

Tsai Y. J. and Huang C. H. (1972) Evaiuation of varying meteorological parameters on cooling-tower plume behavior. In *Symposium on Atmospheric Diffusion and Air Pollution*, American Meteorological Society, Boston, Mass., 408–411.

Viollet M. P-L. (1977) Étude de jets des courants traversiers et dans des milieux stratifies. Doctoral thesis, l'Université Pierre et Marie Curie, Paris.

Weil J. (1974) The rise of moist buoyant plumes. *J. appl. Met.* **13**, 435–443.

Winiarski L. and Frick W. (1976) Cooling tower plume model. USEPA Ecological Research Series, EPA-600/3-76-100, USEPA, Corvallis, Oregon.

Winiarski L. and Frick W. (1978) Methods of improving plume models, cooling tower environment—1978. *Proc., Power Plant Siting Commission, Maryland Dept. of Natural Resources*, PP5P-CPCTP-22, WRRC Special Report No. 9.